Mon. Not. R. Astron. Soc. **000**, 1–?? (2006) Printed 8 May 2008 (MN LATEX style file v2.2)

On the peculiar properties of the narrow-line quasar PG 1543+489

Cristian Vignali,[1,2⋆] Enrico Piconcelli[3⋆], Stefano Bianchi[4,5⋆] and Giovanni Miniutti[6,7⋆]

[1] *Dipartimento di Astronomia, Università degli Studi di Bologna, Via Ranzani 1, I–40127 Bologna, Italy*
[2] *INAF – Osservatorio Astronomico di Bologna, Via Ranzani 1, I–40127 Bologna, Italy*
[3] *INAF – Osservatorio Astronomico di Roma, Via Frascati 33, I–00040 Monteporzio Catone, Italy*
[4] *Dipartimento di Fisica, Università degli Studi di Roma Tre, Via della Vasca Navale 84, I–00146 Roma, Italy*
[5] *ESA – European Space Astronomy Center, Apartado 50727, E–28080 Madrid, Spain*
[6] *Institute of Astronomy, Madingley Road, Cambridge CB3 0HA, UK*
[7] *Laboratoire APC, UMR 7164, 10 rue A. Domon et L. Duquet, 75205 Paris, France*

Accepted 2008 May 7. Received 2008 May 7; in original form 2008 March 21

ABSTRACT

We present the analysis of four XMM-*Newton* observations of the narrow-line quasar PG 1543+489 at z=0.400 carried out over a rest-frame time-scale of about three years. The X-ray spectrum is characterized by a broad, relativistic iron K_α emission line and a steep photon index, which can be both explained by a ionized reflection model, where the source of X-ray photons is presumably very close to the black hole. If this were the case, strong light-bending effects are expected, and actually they provide the most plausible explanation for the large equivalent width (EW=3.1$\pm$0.8 keV in the source rest frame) of the iron line. Although the light-bending model provides a good description of the X-ray data of PG 1543+489, it is not possible to rule out an absorption model, where obscuring matter partially covers the X-ray source. However, the apparent lack of variations in the properties of the absorber over the time-scale probed by our observations may indicate that this model is less likely.

Key words: quasars: general — quasars: individual: PG 1543+489— galaxies: nuclei — galaxies: active

1 INTRODUCTION

The Palomar-Green (PG) quasars (Schmidt & Green 1983) represent one of the best studied samples of Active Galactic Nuclei (AGN). Because of their relatively high X-ray luminosities, over the last decade their properties have been widely investigated by almost all the X-ray satellites, from *ROSAT* (e.g., Laor et al. 1997) to *ASCA* (e.g., George et al. 2000), *BeppoSAX* (e.g., Mineo et al. 2000) and, lastly, XMM-*Newton* (Porquet et al. 2004; Piconcelli et al. 2005; Jiménez-Bailón et al. 2005; Brocksopp et al. 2006). In particular, the high-energy throughput of the XMM-*Newton* EPIC instruments have recently allowed a detailed investigation of their spectral properties in the $\approx$ 0.3–10 keV band (e.g., Piconcelli et al. 2005; Jiménez-Bailón et al. 2005), showing the ubiquitous presence of soft excesses and iron K_α emission lines, as well as, in half of the sample, of warm absorbers.

Here we present the X-ray analysis of the XMM-*Newton* spectrum of PG 1543+489, a narrow-line quasar (NLQ) [the full width at half maximum (FWHM) of the H_β line is 1630 km s^{-1} (Aoki, Kawaguchi & Ohta 2005)] at a redshift of z=0.400. According to optical and ultra-violet mass scaling, this quasar is likely characterized by a (1–2.4)$\times10^8$ $M_\odot$ black hole (D'Elia, Padovani & Landt 2003; Vestergaard & Peterson 2006); a even larger black hole mass was estimated by Brocksopp et al. (2006) using a spectral energy distribution (SED) fitting approach. Furthermore, from the measured $\lambda L_{5100\text{Å}}$ ($\approx 10^{45.6}$ erg s^{-1}; Aoki et al. 2005) and adopting the bolometric correction for broad-line (Type 1) quasars reported in Richards et al. (2006), we can estimate a remarkably high Eddington ratio [defined as L_{bol}/L_{Edd}, where L_{bol} is the bolometric luminosity and L_{Edd}=(1.3–3.1)$\times10^{46}$ erg s^{-1} is the Eddington luminosity] of $\approx$ 1.3–3.7 for PG 1543+489 (vs. $\approx$ 2.3 of Baskin & Laor 2005). This value, similar to that obtained by Aoki et al. (2005), appears significantly higher than the one estimated from the observed 2–10 keV luminosity ($\approx 1.1\times10^{44}$ erg s^{-1}; see §2.4) using the Elvis et al. (1994) average SED of broad-line quasars, which is $\approx$ 0.1–0.3. The difference in the estimates of the bolometric luminosity (from the $\lambda L_{5100\text{Å}}$ and the 2–10 keV luminosity) can be partially overcome by assuming Eq. 21 in Marconi et al. (2004; see their section 3.2). In this case, the bolometric luminosity derived using the B−band luminosity is a factor of $\approx$ 4.8 lower than the one obtained by Richards et al. (2006) from the $\lambda L_{5100\text{Å}}$. We expect that in objects with large Eddington ratios the metallicity is considerably high (e.g., Shemmer et al. 2004; Netzer & Trakhtenbrot 2007), as actually observed in PG 1543+489 (Aoki et al. 2005).

⋆ E-mail: cristian.vignali@unibo.it (CV); piconcelli@mporzio.astro.it (EP); bianchi@fis.uniroma3.it (SB); miniutti@apc.univ-paris7.fr (GM).

Table 1. XMM-*Newton* observation log.

Quasar Name	RA (J2000.0)	DEC (J2000.0)	z	N_H[a]	Observation OBS_ID	Start Date	Net Exposure Time[b] / Source Counts[c] / Extr. Radius[d] pn	MOS1	MOS2
PG 1543+489	15 45 30.2	48 46 09.1	0.400	1.59	0153220401	2003 Feb 08	9.3/3010/27	11.6/860/24	11.8/910/24
					0505050201	2007 Jun 09	6.6/3530/45	8.8/1030/30	8.8/950/30
					0505050701	2007 Jun 15	6.7/3160/35	8.8/950/25	8.7/920/25
					0505050301	2007 Jun 17	10.4/4730/25	13.6/1520/25	13.6/1480/25

[a] Neutral Galactic absorption column density in units of 10^{20} cm^{-2} obtained from Dickey & Lockman (1990). [b] The exposure times (ks) have been corrected for the high-background intervals (see §2.1 for details), which still contaminate significantly the data of OBS_ID=0505050301. [c] The source counts are reported in the 0.3–10 keV band. [d] Source extraction radius (arcsec).

A peculiarity of PG 1543+489 is the blueshift of the [O III] 5007Å line (1150 km s^{-1} with respect to the systemic velocity of the galaxy) and the blue asymmetry of its profile (Aoki et al. 2005). The large [O III] blueshift of the so-called "blue outliers"[1] (to which PG 1543+489 belongs) has been theoretically interpreted as the result of an outflow whose receding part is obscured by an optically thick accretion disc (Zamanov et al. 2002) or by a scenario in which the narrow-line region clouds are entrained in a decelerating wind, possibly linked to the high Eddington ratio typical of the "blue outliers" (Komossa et al. 2008). The amount of blueshift does not appear to correlate with the Eddington ratio; however, there is a clear connection between being a "blue outlier" and the Eddington ratio itself (Aoki et al. 2005); this issue clearly needs further and extended investigations. Interestingly, PG 1543+489 has the largest [O III] blueshift (relative to H_β) among the 280 broad-line AGN in the sample of Marziani et al. (2003a); although outflow phenomena have been reported in other narrow-line Seyfert 1 galaxies (NLS1s) and NLQs, to our knowledge PG 1543+489 shows the most extreme value of blueshift among AGN not classified as broad absorption-line (BAL) quasars. The remarkably strong asymmetric profile of the blueshifted C IV emission line (Baskin & Laor 2005) provides a further indication that PG 1543+489 is an intriguing source with a large Eddington ratio.

Previous observations in the soft and hard X-rays have shown that NLS1s and NLQs have typically steeper X-ray spectra [in both the soft (e.g., Boller, Brandt & Fink 1996) and hard X-ray band (e.g., Brandt, Mathur & Elvis 1997)] than "normal" broad-line quasars, whose photon index is $\Gamma \approx 1.9$–2.0 in the 2–10 keV band (e.g., Reeves & Turner 2000; Page et al. 2003) and independent on the source redshift and luminosity (e.g., Piconcelli et al. 2003; Vignali et al. 2005; Shemmer et al. 2005; Page et al. 2005; but see also Dai et al. 2004 and Saez et al. 2008 for different results). In Type 1 AGN, a well established anti-correlation between the photon index and the H_β FWHM exists both in the soft and hard X-ray band (e.g., Laor et al. 1994, 1997; Brandt et al. 1997). Based on the reasoning that eventually led to the Kaspi et al. (2000) results, the FWHM of the H_β line was suggested to be an accretion rate indicator in broad-line AGN (e.g., Boroson & Green 1992; Brandt & Boller 1998), i.e., objects with narrower H_β lines are thought to accrete at a higher fraction of the Eddington limit. On the basis of this finding, Reeves & Turner (2000) explained the steepening of the X-ray spectrum as due to a larger Compton cooling of the hard X-ray emitting corona (e.g., Pounds, Done & Osborne 1995; see also Puchnarewicz et al. 1995).

[1] According to the definition of Marziani et al. 2003b, a "blue outlier" is a source where $\Delta v_{r\ [OIII]} = v_r([OIII]\lambda5007) - v_r(H_\beta) \lesssim -300$ km s^{-1}, where v_r is the radial velocity as measured on the Fe II–subtracted spectrum.

In this context, the X-ray observations of PG 1543+489 are meant to provide a powerful insight on the emission in the innermost regions of the quasar; the presence of a steep photon index, as indicated by the *ASCA* observation (George et al. 2000), coupled with the narrow H_β emission line, would imply a high accretion rate for this source (see the recent works by Shemmer et al. 2006, 2008 and references therein), likely related to the outflow phenomena.

Hereafter we adopt H_0=70 km s^{-1} Mpc^{-1} in a Λ-cosmology with Ω_M=0.3 and Ω_Λ=0.7 (Spergel et al. 2003).

2 XMM-NEWTON OBSERVATIONS OF PG 1543+489

The XMM-*Newton* data reported in this paper consist of four observations, the first of which (dated Feb. 2003) being retrieved from the archive and published by Matsumoto, Leighly & Kawaguchi (2006) and Brocksopp et al. (2006). The remaining three observations were obtained in XMM-*Newton* AO6 call for proposals, and the source was observed in June 2007. The observation log of all the XMM-*Newton* observations of PG 1543+489 is reported in Table 1.

2.1 EPIC data reduction

The XMM-*Newton* data were processed using standard SAS V7.0.0 (Gabriel et al. 2004) and FTOOLS tasks. The event files were filtered to include events with pattern $\leqslant$4 and $\leqslant$12 for the pn and MOS instruments, respectively, over the energy range 0.3–10 keV. High-background intervals are present in all of the observations; the procedure to obtain a good compromise between clean event files and relatively good statistics consists of using the script *xmm-light_clean.csh* [2] which performs a recursive 3σ cleaning on the lightcurves in the 10–15 keV energy range (binned in 100-s intervals) until the mean count rate per bin is constant. The goodness of this cleaning process (proven to be effective in past observations) has been checked on the resulting lightcurves and images, adopting different bin intervals, and by comparison with other cleaning methods (e.g., adopting the procedure reported in Baldi et al. 2002), confirming the achievement of a relatively good final result. The only exception is the last observation carried out in 2007 (OBS_ID=0505050301), which still shows the presence of significant residual flares after the cleaning process, hampering a good analysis of the data. For this reason, the data of this observation will not be considered further. The final "cleaned" exposure times are reported in Table 1.

To extract X-ray spectra, we used variable source-extraction

[2] Available at http://www.sr.bham.ac.uk/xmm2/scripts.html.

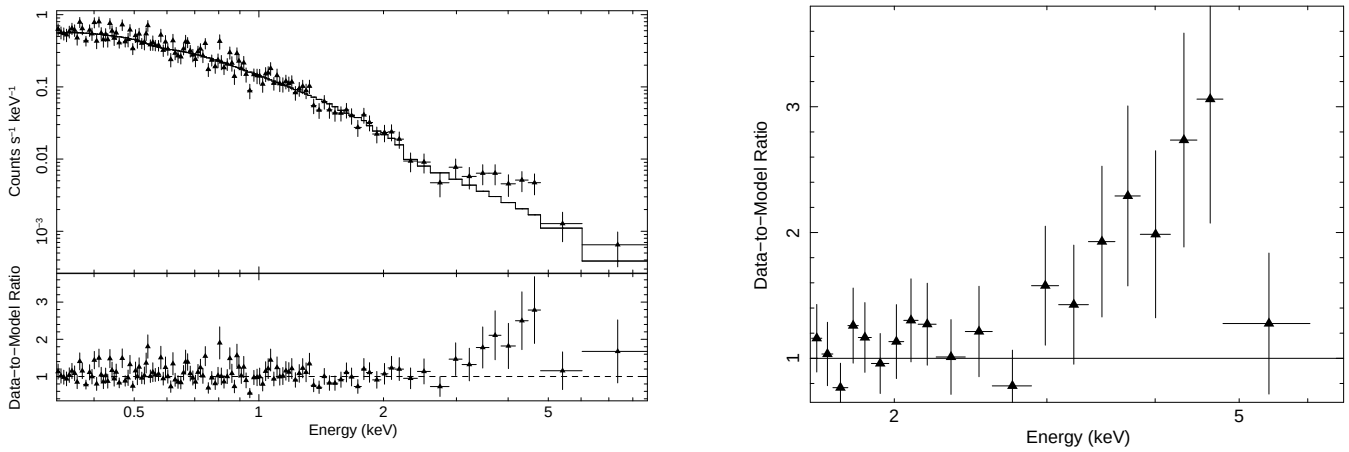

Figure 1. *(Left panel)* Fitting to the archival pn data (OBS_ID=0153220401) over the $\approx$ 0.3–10 keV energy range using a power-law model and Galactic absorption. The data-to-model ratios are shown in the bottom panel in units of σ. *(Right panel)* Close-up of the deviations (in units of σ) in the $\approx$ 1.5–7 keV band of the observed EPIC pn data adopting a power-law model fitted to the (0.3–3 keV) + (6–10 keV) range and extrapolated to the whole energy interval.

aperture radii to maximize the signal-to-noise (S/N) ratio over the entire 0.3–10 keV energy range and obtain good counting statistics for moderate-quality spectral analysis. Radii vary from 27 to 45 arcsec for the pn, and from 24 to 30 arcsec for the two MOS cameras. The background was taken from circular regions, in the same chip (to avoid significant spatial variations across the detector) and close to PG 1543+489 (without being contaminated by the target itself) with radii of 90″. The adoption of multiple background regions did not provide significantly different results. The redistribution matrix files (RMFs, which include information on the detector gain and energy resolution), and the ancillary response files (ARFs, which include information on the effective area of the instrument, filter transmission and any additional energy-dependent efficiencies) were created with the SAS tasks RMFGEN and ARFGEN, respectively. The resulting pn (MOS) spectra were grouped with a minimum of 20 (15) counts per bin using the task GRPPHA, in order to apply the χ^2 statistic, and fitted with XSPEC V12.4.0 (Arnaud 1996).

During each observation, the flux level in the soft (0.5–2 keV) and hard band (2–10 keV) did not show significant (i.e., above the $\approx$ 20 per cent) variations, according to a χ^2 test.

2.2 Optical Monitor data

In order to obtain information on the broad-band (UV to X-ray) spectral properties of PG 1543+489 (see §3), we used the Optical Monitor (OM) products, which consist of flux densities and magnitudes in selected filters. While for the archival observation only data taken with the UVM2 filter (having an effective wavelength of 2310 Å) are available, all of the other observations have U−band coverage (effective wavelength of 3440 Å), and in the first observation of June 2007 (OBS_ID=0505050201) also the UVM2 filter was operating.

2.3 X-ray spectral analysis

At first, we checked the pn, MOS1 and MOS2 data for consistency (over the $\approx$ 0.3–10 keV band) within each observation, assuming a power-law model, and found generally a good agreement in both the photon index and the overall shape of the residuals among the different EPIC instruments. Some residuals appear evident in the $\approx$ 3–6 keV energy range, being particularly prominent in the pn data (likely because of its higher effective area compared to that of the MOS cameras). As an example, in Fig. 1 (left panel) we report the fitting to the pn data with a power-law model and Galactic absorption using the archival data only, since this observation has subsequently driven the science case of the proposed and awarded 2007 observations. The residuals resemble those expected in case of a broad, relativistic (because of the pronounced red wing) iron line, as suggested by the close-up of the deviations centered on the presumably broad iron feature shown in Fig. 1 (right panel).

Table 2. Counts in EPIC after optimisation of the source extraction regions.

	Opt. Extr. Region (arcsec)			Net Source Counts		
OBS_ID	pn	MOS1	MOS2	pn	MOS1	MOS2
0153220401	16	26	21	2560	840	840
0505050201	18	40	24	2830	1080	910
0505050701	16	38	25	2590	1030	910

The source extraction regions have been chosen to optimise the signal-to-noise ratio in the 2–10 keV band (see §2.3 for details); source counts are reported over the entire 0.3–7 keV energy range.

Given the necessity of a proper investigation of the hard-band spectral complexities of PG 1543+489, we decided to re-extract the source spectra from all EPIC instruments adopting an "optimised" radius for each source extraction region (see Table 2). This radius was chosen to maximize the S/N ratio over the 2–10 keV band using the task *eregionanalyse* within the SAS. The results from this task were checked against different choices of the background regions. The spectra were binned with a minimum of 20 counts per bin in all pn observations and 15 counts per bin in all MOS data. Good source signal is present in the $\approx$ 0.3–7 keV band, then at higher energies the background starts providing a relevant contribution in the spectral fitting. For this reason, to provide robust spectral results, the analyses presented in the following are produced in this energy range, at the expense of a total of $\approx$ 150 counts with respect to the number of counts in the 0.3–10 keV band.

Despite the observed source flux variations over the rest-frame time-scale of $\approx$ 3 years probed by our observations (the 0.5–10 keV flux was $\approx 5 \times 10^{-13}$ erg cm^{-2} s^{-1} in 2003 and increased by $\approx$ 50% in the observations carried out in 2007), the X-ray spectral shape of PG 1543+489 does not appear to vary dramatically

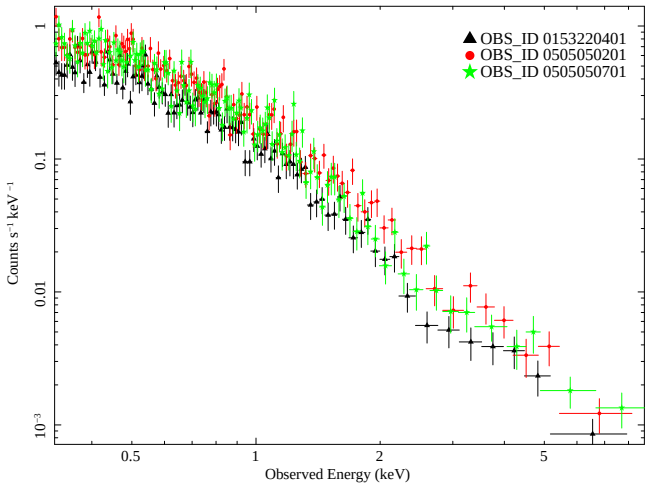

Figure 2. EPIC pn data taken from the three observations reported in Table 2, where the radius of the source extraction regions has been chosen such to maximize the signal-to-noise ratio in the 2–10 keV band (see §2.3 for details).

(see Fig. 2). Motivated by these considerations and in order to increase the significance of our spectral results, we fitted all the X-ray data (see Table 2) simultaneously, leaving the normalisations free to vary to account for the different calibrations (a few per cent) of the EPIC cameras. The spectral analysis presented in the following sections has been carried out on the summed spectra (i.e., one spectrum for three pn datasets and similarly for the MOS1 and MOS2 instruments) obtained combining the individual source (background) spectra with the tool *mathpha* and averaging the RMF and ARF matrices by the relative exposure times using the FTOOLS *addrmf* and *addarf*, respectively. This choice, accurately checked against simultaneous fitting of all the individual pn and MOS spectra, was found to produce reliable X-ray spectral results and, overall, allows a more direct visualization of the spectral findings in case of many datasets.

Hereafter, the quoted errors on the derived model parameters correspond to the 90 per cent confidence level for one interesting parameter (i.e., $\Delta\chi^2 = 2.71$; Avni 1976), if not stated otherwise; all spectral fits include absorption due to the line-of-sight Galactic column density of $N_{\rm H} = 1.59 \times 10^{20}$ cm^{-2} (Dickey & Lockman 1990), and Anders & Grevesse (1989) abundances are assumed.

Similarly to the situation illustrated in Fig. 1, a single power-law model is not able to reproduce the data of all the EPIC data, leaving strong residuals in the hard band (see Table 3, model (a) and Fig. 3). The inclusion of a broad line, either modelled with a Gaussian (model ZGAUSS in XSPEC; model (b) in Table 3) or a relativistic component (models DISKLINE and LAOR in the case of a black hole in the Schwarzschild and Kerr metric, respectively – models (c) and (d) in Table 3; Fabian et al. 1989; Laor 1991) improves the fit by $\Delta\chi^2 \approx$19–50 for 2–3 additional degrees of freedom (the line energy, width and normalisation in the ZGAUSS model, and line energy and normalisation in the relativistic models, where the inner radius of the accretion disc was fixed to the minimum radius allowed by the two metrics and the emissivity index was left to its default value in the LAOR model). Although the highest improvement, in terms of χ^2, is obtained using a Gaussian iron line, the width of this line ($\sigma = 2.98^{+4.55}_{-1.14}$ keV), coupled with its centroid energy (unconstrained), suggests that a more accurate spectral parameterization (e.g., a relativistic feature) is needed to properly reproduce the data. Using the LAOR model (c), the improvement in

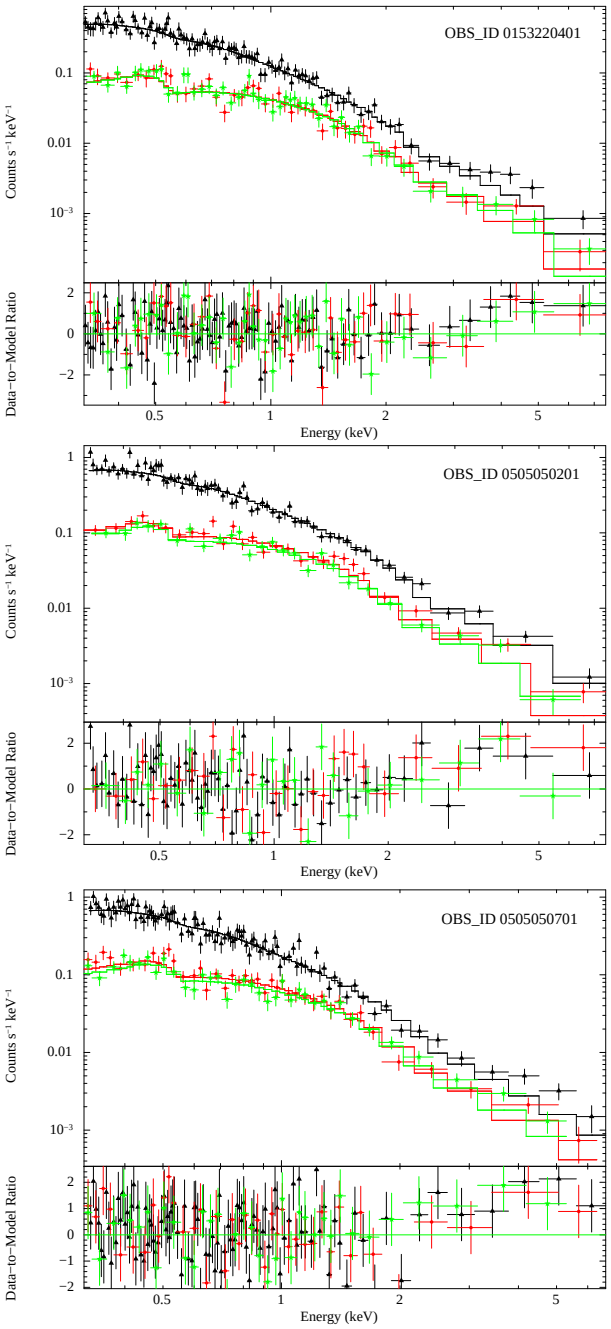

Figure 3. Fitting to the pn (triangles), MOS1 (filled circles) and MOS2 (stars) spectral data of the three observations over the ≈ 0.3–7 keV energy range using a power-law model and Galactic absorption. The data-to-model ratios are shown in the bottom panels in units of σ.

the spectral fitting corresponds to the >99.999 per cent (according to the F-test) with respect to the single power-law model; since the iron line normalisation was allowed to be negative in the spectral fitting, the F-test can still be considered a reliable method to derive the statistical significance of the line (see Protassov et al. 2002). The best-fitting rest-frame energy, $6.7^{+0.2}_{-0.5}$ keV in the case of a LAOR line, is consistent, within the errors, with that obtained in case of a DISKLINE, with the former model being preferred on a statistical basis (Table 3) and from visual inspection of the data-to-model ratios. The line energy is consistent with neutral iron up to Fe XXV. The equivalent width (EW) of the relativistic line

Table 3. X-ray spectral results of the EPIC pn and MOS data.

Model (1)	Γ (2)	E (3)	EW (4)	ξ (5)	N_H (6)	Cov. Fract (7)	χ^2/dof (8)
(a)	2.70±0.03						495.5/442
(b)	$2.81^{+0.07}_{-0.04}$	4.09 unc.	$2.35^{+5.61}_{-1.23}$				445.0/439
(c)	2.75±0.03	$6.71^{+0.21}_{-0.53}$	3.09±0.84				458.9/440
(d)	$2.72^{+0.02}_{-0.03}$	6.33±0.11	$1.12^{+0.20}_{-0.60}$				476.4/440
(e)	$2.35^{+0.01}_{-0.02}$			> 6760			460.8/441
(f)	2.78±0.04				$2.12^{+1.91}_{-0.89}$	$0.53^{+0.12}_{-0.10}$	445.1/440

The relative normalisation of the MOS cameras with respect to the pn is 1.03–1.04 in all the spectral fittings presented here. (1) Reference for the model adopted in the spectral fitting (see below and §2.3 for details); (2) Photon index over the 0.3–7 keV bandpass; (3) Rest-frame energy of the line (keV); (4) Rest-frame equivalent width of the line (keV); (5) Ionization parameter $\xi = \frac{4\pi F_{\rm tot}}{n_{\rm H}}$ (erg cm s^{-1}), where $F_{\rm tot}$ is the total illuminating flux and $n_{\rm H}$ is the hydrogen number density (part cm^{-3}) of the illuminated slab; (6) Rest-frame column density (in units of 10^{23} cm^{-2}); (7) Covering fraction of the absorbing matter; (8) Goodness of the fit in terms of χ^2/(number of degrees of freedom, d.o.f.).
Adopted models: (a) powerlaw; (b) powerlaw and broad Gaussian iron line; (c) powerlaw and relativistic (LAOR) iron line; (d) powerlaw and relativistic (DISKLINE) iron line; (e) ionized reflection (REFLION model), convolved with a relativistic blurring kernel from the Laor (1991) code (KDBLUR); (f) powerlaw plus partial covering absorption.

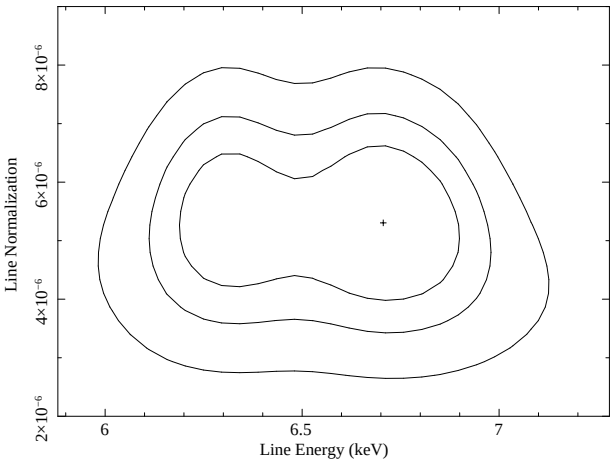

Figure 4. 68, 90 and 99 per cent confidence contours showing the rest-frame energy vs. photon flux of the relativistic iron emission line (LAOR model in XSPEC).

(EW=3.1±0.8 keV in the source rest frame) is much larger than that measured in case of detection of broad features by *ASCA* and XMM-*Newton* for a sample of nearby AGN (EW≈ 230–250 eV; Nandra et al. 1997; Guainazzi, Bianchi & Dovčiak 2006); we defer a more exhaustive discussion on possible causes of this strong feature in §3. The rest-frame line energy vs. normalisation in the LAOR model, shown in Fig. 4, is likely suggestive of a more complex modeling for PG 1543+489.

The power-law photon index does not vary significantly with the inclusion of a broad feature, being $\Gamma \approx 2.7-2.8$, in agreement with that derived from *ASCA* data. Although warm absorbers and soft excesses are often detected in PG quasars (e.g., Reynolds 1997; Porquet et al. 2004; Piconcelli et al. 2005), we must note that there is no strong indication that the main features of warm absorbers (i.e., the O VII and O VIII absorption edges and the unresolved transition array, UTA; e.g., Piconcelli et al. 2005) are present in the EPIC spectra; furthermore, the source redshift (z=0.400) is such to plausibly move a significant fraction of any additional soft component below the energy interval where the EPIC instruments are mostly sensitive.

Given the recent claims that NLS1 and NLQ X-ray spectra could be reflection-dominated (e.g., Fabian et al. 2002, but see also Done 2007) and the convincing results obtained for some AGN of this class, where the whole X-ray continuum emission and iron K_α line are well explained in terms of reflection (e.g., Fabian et al. 2004; Gallo et al. 2004a and references therein), we tried to fit all the data using a ionized reflection model (REFLION[3] into XSPEC; Ross & Fabian 2005), which incorporates both line emission with Compton broadening and reflection continuum, convolved with a relativistic blurring kernel from the Laor (1991) code (KDBLUR into XSPEC; model (e) in Table 3). This spectral parameterization is well suited to represent the light-bending model, where the presence of a reflection-dominated spectrum is interpreted as due to strong light-bending effects at work close to the black hole (Miniutti & Fabian 2004; see §3). The iron abundance was fixed to solar, and the other spectral parameters frozen to their default values. The quality of the fit ($\chi^2/d.o.f. = 460.8/441$) is similar to that obtained in the case of a relativistic iron line plus a steep X-ray continuum, the only difference being a flatter photon index (Γ=$2.35^{+0.01}_{-0.02}$) and, likely, a more physical description of the X-ray emission of PG 1543+489; the spectrum is shown in Fig. 5

Unfortunately, the quality of the data does not allow us to constrain the ionization parameter ($\xi = \frac{4\pi F_{\rm tot}}{n_{\rm H}} > 6760$ erg cm s^{-1}, where $F_{\rm tot}$ is the total illuminating flux and $n_{\rm H}$ is the hydrogen number density) and to distinguish, on the basis of the χ^2 and the inner radius of the accretion disc (once left free to vary), between a maximally spinning black hole and a non-spinning Schwarzschild black hole. In these highly ionised conditions, the disc acts like a perfect reflector (see Ross & Fabian 2005), whose main properties are a power-law similar to the incident one, a modest Compton hump, and a "smeared" iron line and edge, due to the effects of Comptonization. For this reason, it is difficult to place constraints on the relative strength of the reflection continuum with respect to the incident powerlaw, which is broadly constrained in the range 1.5–6.0

[3] Available at http://heasarc.gsfc.nasa.gov/docs/xanadu/xspec/models/reflion.html as external table.

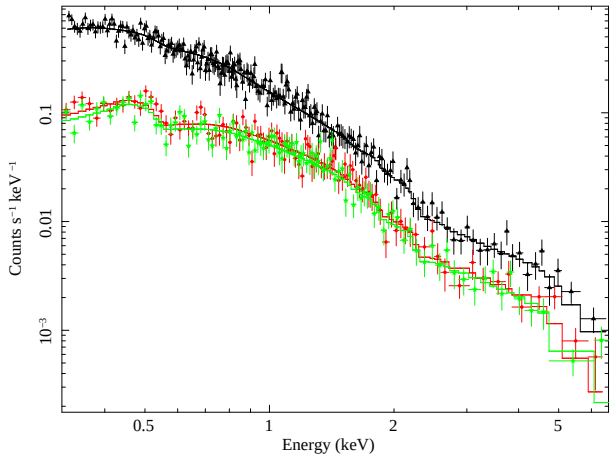

Figure 5. pn (triangles), MOS1 (filled circles) and MOS2 (stars) spectral data of the three observations discussed in §2.3 fitted with a ionized reflection model convolved with a relativistic blurring kernel from the Laor code (model (e) in Table 3).

for solar abundances. Although the optical spectrum indicates iron over-abundance (see §2.3 of Aoki et al. 2005), we note that, from an X-ray perspective, a slightly better statistical result (improvement by $\Delta\chi^2 \approx 9$ for one additional degree of freedom with respect to the model with iron abundance fixed to solar) is achieved leaving the iron abundance free to vary in the spectral fitting (and the Fe abundance relative to the solar value is $0.64^{+0.26}_{-0.25}$).

We also note that the iron edge at $\approx$ 7.1 keV or sharp drop in the continuum flux observed in some NLS1s (e.g., Boller 2004; Gallo et al. 2004b) and interpreted in terms of reflection cannot be investigated by the current data, because at these high energies the source and background signals become approximately comparable (see §2.3).

Finally, we tried to model the spectrum of PG 1543+489 using a partial-covering model (model (f)) instead of a reflection component. This spectral fitting provides a statistically better result ($\chi^2/d.o.f. = 445.1/440$), a steep photon index ($\Gamma = 2.78 \pm 0.04$) and a covering fraction (i.e., the fraction of the nuclear source covered by the absorber) of $0.53^{+0.12}_{-0.10}$. The derived rest-frame column density ($N_H = 2.12^{+1.91}_{-0.89} \times 10^{23}$ cm^{-2}) appears difficult to reconcile with the apparent lack of extinction in the optical/UV spectrum of PG 1543+489 (e.g., Baskin & Laor 2005) but could be explained assuming a dust-to-gas ratio largely below the Galactic value (e.g., Maiolino et al. 2001). In this model, where the absorber must be close to the X-ray emitting region, possibly within the sublimation radius (thus explaining the low extinction), we would expect to observe significant variations in the parameters of the partial covering model over the three observations used in the spectral fitting. Although the spectral constraints from the individual observations are relatively poor, we find that in the archival observation and in the two 2007 observations the column density is $N_H = 3.2^{+5.5}_{-2.0} \times 10^{23}$ cm^{-2} and $N_H = 1.2^{+1.3}_{-0.5} \times 10^{23}$ cm^{-2}, and the covering fraction 0.59 ± 0.27 and $0.53^{+0.11}_{-0.14}$, respectively. Therefore, within the statistical uncertainties, it seems that no significant variations in the absorber occur over a rest-frame time-scale of $\approx$ 3 years, which might cast some doubts on the physical reliability of this model. On the other hand, in the framework of the light-bending model, a reduced variability of the reflection component with respect to the continuum can be explained. If the continuum variability is not entirely intrinsic but is mainly due to changes in the location of the primary source of hard X-rays, light-bending effects close to the central massive black hole predict little variability of the spectral components reprocessed by the accretion disc (Miniutti & Fabian 2004).

In all the models mentioned above, the inclusion of a narrow (σ=10 eV) iron K_α line at 6.4 keV (rest-frame EW$<$450 eV) is not required by the data.

2.4 Long-term X-ray flux variability of PG 1543+489

In the attempt to evaluate the long-term behaviour of PG 1543+489, we analysed the *ASCA* on-axis observation of this quasar (see George et al. 2000), using the products available at the TARTARUS database[4]), and an off-axis observation with *Chandra*, coupled with the three XMM-*Newton* observations presented in the previous section. From *ASCA* to the archival XMM-*Newton* observation, over a time-scale of $\approx$6 years ($\approx$4.3 years in the source rest frame), the 2–10 keV source flux has changed by a factor of $\approx$3.5 (from ≈ 5.1–5.3×10^{-13} erg cm^{-2} s^{-1} in the *ASCA* observation to $\approx 1.7 \times 10^{-13}$ erg cm^{-2} s^{-1} in the first XMM-*Newton* observation, which corresponds to a rest-frame 2–10 keV luminosity of $\approx 1.1 \times 10^{44}$ erg s^{-1}), with no evidence for X-ray spectral variability. Unfortunately, the 2002 *Chandra* observation does not provide enough counts ($\approx$ 220) for a detailed X-ray spectral fitting, and the spectral analysis is limited in the energy range $\approx$ 0.5–4 keV. Within the uncertainties, the constraints on the photon index obtained by *Chandra* are consistent with our XMM-*Newton* results, and the extrapolated 2–10 keV flux is intermediate between those measured by *ASCA* and XMM-*Newton* (archival observation). In 2007, the source 2–10 keV flux increased to $\approx 2.7 \times 10^{-13}$ erg cm^{-2} s^{-1} (OBS_ID=0505050201) and by a similar factor in the 0.5–2 keV band, and became $\approx 2.4 \times 10^{-13}$ erg cm^{-2} s^{-1} in the last analysed XMM-*Newton* observation (OBS_ID=0505050701).

3 DISCUSSION

From a broad-band perspective, the combined analysis of EPIC and OM data of PG 1543+489 allows us a simultaneous study of its SED, parameterized by α_{ox}, the slope of the hypothetical powerlaw connecting the rest-frame wavelengths of 2500 Å and 2 keV and defined as

$$\alpha_{ox} = \frac{\log(f_{2\ \mathrm{keV}}/f_{2500\ \text{Å}})}{\log(\nu_{2\ \mathrm{keV}}/\nu_{2500\ \text{Å}})} \qquad (1)$$

where $f_{2\ \mathrm{keV}}$ and $f_{2500\ \text{Å}}$ are the flux densities at rest-frame 2 keV and 2500 Å, respectively. In this regard, the derived α_{ox} values (-1.64 for the archival observation, -1.45 and -1.47 for the 2007 observations analysed in §2.3[5]) are fully consistent with those expected on the basis of the known anti-correlation between this spectral index and the 2500 Å luminosity (using the most up-to-date parameterization reported in Just et al. 2007). Therefore, at

[4] See http://tartarus.gsfc.nasa.gov/.

[5] For the 2007 observations, in the α_{ox} calculation we used the U$-$band flux density, since this filter at z=0.40 approximately samples the rest-frame wavelength of 2500 Å, while for the archival observation, the flux density obtained from the UVM2 filter was extrapolated assuming the UV slope reported in Matsumoto et al. (2006); our result is consistent with Matsumoto et al. findings.

least in the UV-to-X-ray energy range, the broad-band properties of PG 1543+489 do not appear to be unusual.

From an X-ray point-of-view, the spectrum of PG 1543+489 appears characterized by a steep photon index and a strongly skewed, relativistic iron line, both accounted for by a ionized reflection model. There are indications that the former spectral result may be related to the high accretion rate of the source (Aoki et al. 2005; Baskin & Laor 2005), as actually found in most of the NLS1s and NLQs (e.g., Boroson 2002). As a further support to such indication, Shemmer et al. (2006), using a sample of 30 quasars up to redshift ≈ 2, have shown that the photon index depends primarily on the source accretion rate; this correlation is more robust than that obtained for Γ vs. FWHM(H_β), i.e., sources with steeper X-ray spectra (both in the soft and hard X-rays) have typically narrower H_β emission lines (e.g., Laor et al. 1994, 1997; Brandt et al. 1997), as actually observed also in PG 1543+489.

As a non-secondary effect/indication of the high accretion rate of this source, there is evidence for a strong blueshift and asymmetric profile in the [O III] 5007Å and C IV 1459Å emission lines (Aoki et al. 2005; Baskin & Laor 2005); a high-ionization, optically thin wind, propagating outward the broad-line region and caused by the radiation pressure of the quasar represents a viable explanation (Marziani et al. 2003b), as well as a scenario whereby the narrow-line region clouds are entrained in a decelerating wind (Komossa et al. 2008). This result finds support from the dependence of the amount of blueshift vs. the source optical luminosity in a sample of quasars with similar properties to those of PG 1543+489 (Aoki et al. 2005).

The presence of a relativistic iron line places this quasar among the small number of luminous AGN where such feature has been detected so far. In addition to those Seyfert-like AGN that "historically" (i.e., since *ASCA* and *RXTE* observations) were known to doubtlessly show relativistic iron lines (e.g., MCG−6−30−15, Tanaka et al. 1995; NGC 3516, Nandra et al. 1999; IRAS 18325−5926, Iwasawa et al. 1996; MCG−5−23−16, Weaver, Krolik & Pier 1998), over the last few years XMM-*Newton* and *Chandra* good-quality spectral data have allowed detailed investigations of the presence of relativistic features in a sizable number of AGN (e.g., Porquet & Reeves 2003; Miniutti & Fabian 2006; Porquet 2006; Piconcelli et al. 2006 and references therein; Longinotti et al. 2007; Miniutti et al. 2006; Krumpe et al. 2007; Schartel et al. 2007), also at moderately high redshifts (e.g., Comastri, Brusa & Civano 2004; Chartas et al. 2007), and have enabled relevant statistical analyses (Guainazzi et al. 2006; Nandra et al. 2006; Inoue, Terashima & Ho 2007). From these studies, ≈ 40 per cent of the XMM-*Newton* AGN with more than 10000 counts in the 2–10 keV band have broad iron features (Guainazzi et al. 2006), although the situation may be more complex and foresee the presence of complex absorption (e.g., Nandra et al. 2007).

Although further data may be required to provide better constraints on the ionization of the continuum and, possibly, on the line parameters, it is interesting to note that this is the first time that such line is detected in PG 1543+489: the *ASCA* observation showed only marginal evidence for the presence of a broad iron line, probably due to the higher background level of the *ASCA* observation and lower effective area of its instruments. We also note that the line was not detected in the analysis of the archival XMM-*Newton* observation carried out by Brocksopp et al. (2006) and Matsumoto et al. (2006), with an upper limit to a narrow iron K_α line being 800 eV according to the latter authors. It seems plausible that the data reduction procedure and cleaning performed by the other authors are different from ours. This possibility is confirmed by the much larger statistical uncertainties that Brocksopp et al. (2006) quote in their spectral fittings than those presented in this work (§2.3), probably caused by a less effective subtraction of the flaring-background intervals (as apparent from their Fig. 1) and by our adopted strategy to enhance the S/N ratio in the hard band via the source extraction radius optimisation (§2.3). Moreover, the availability of multiple XMM-*Newton* observations of PG 1543+489 showing a similar spectral behaviour provides further support to our results.

A possible cause of concern is the large EW of the iron line (EW=3.1±0.8 keV in the source rest frame), much larger than typically observed in local Seyfert galaxies and quasars and among the largest EWs ever found in AGN (see, for comparison, Fig. 2 of Guainazzi et al. 2006). Plausible explanations include (1) significant iron overabundance, (2) reflection-dominated spectrum which, even with solar Fe abundance, yields to a self-consistent line EW with respect to its own reflection continuum, (3) matter partially covering the X-ray source. Although iron over-abundance is present in the optical spectrum of PG 1543+489 (Aoki et al. 2005), the fact that the iron line intensity grows logarithmically with the iron abundance (Matt, Fabian & Reynolds 1997) would require an extremely high abundance to account for the observed iron K_α line EW. Therefore, this hypothesis appears unlikely.

The second hypothesis, the possibility that the X-ray spectrum is reflection-dominated, appears the most plausible, although more accurate spectral data are required to provide a more robust and convincing support to it. According to recent literature, the presence of a reflection-dominated spectrum can be associated with strong light-bending effects at work close to the black hole (Miniutti & Fabian 2004). In this model, strong light bending is expected if the primary source is located close to the central black hole and illuminates the inner regions of the accretion disc. In this situation, almost all of the radiation emitted by the source is bent onto the disc rather than escaping to the observer. In general, the relative fraction of reflected vs. observed power-law flux depends on the height of the source above the disc (e.g., see Miniutti et al. 2003; Miniutti, Fabian & Miller 2004; Crummy et al. 2005; Ponti et al. 2006). Given the good fit to the data obtained using a ionized reflection model convolved with a relativistic blurring kernel from the Laor (1991) code, the source of X-ray photons should be located very close to the black hole during the XMM-*Newton* observations presented here. This reflection model predicts broad and strong iron lines (also see Dabrowski & Lasenby 2001 for details) when the source is in a relatively low X-ray flux regime, which could be the case for PG 1543+489 in the XMM-*Newton* observations (see §2.4); furthermore, it has provided a plausible explanation for the spectral properties of some NLS1s showing reflection-dominated spectra and, possibly, strong iron lines (e.g., Miniutti & Fabian 2004; Porquet 2006), for the luminous NLQ PHL 1092 (Gallo et al. 2004a) and, recently, for the soft excess of many PG quasars (Crummy et al. 2006). As recently pointed out by Merloni et al. (2006), reflection-dominated spectra could also be produced in a disc consisting of a inhomogeneously heated plasma (hot phase) pervaded by small dense clumps (cold phase), which intercept most of the photons coming from the hot phase. Therefore, while in this model the reflection is related to the clumpy and inhomogeneous nature of the inner disc, in the light-bending model it is due to general relativistic effects (for details, see Malzac, Merloni & Suebsuwong 2006), although any further sign of such effects on the X-ray emission is probably not visible because of the still limited statistics. Unfortunately, the current X-ray data do not allow us to discriminate between these two models.

From a statistical and physical basis, also a partial-covering model (third hypothesis) provides a good description of the X-ray spectral complexities of PG 1543+489. Under some assumptions for the absorbing medium (see §2.3), it is possible to reproduce the optical properties of PG 1543+489, which shows a blue continuum and features related to the broad-line region, with no indications for significant extinction. In this model, if the absorber is in form of clouds close to the nuclear engine, X-ray spectral variability is likely to take place due to orbital motions of the matter around the black hole and/or outflow phenomena (see §1). The lack of any appreciable variations in the properties of the absorber over the time-scale probed by our observations suggests that this model is less likely than the light bending model; however, we note that the large uncertainties in the measurements derived from the individual observations prevent us from obtaining a firm conclusion on this issue.

Over the next years, with the availability of extended observations of NLS1s and NLQs, it would be interesting to understand whether some sort of connection exists between the presence of ionized reflection (related to the closeness of the source of X-ray photons to the black hole in the light-bending model), the accretion rate of the AGN and winds/outflows phenomena.

4 SUMMARY

We have analysed an archival plus proprietary XMM-*Newton* observations of PG 1543+489 (probing a rest-frame time-scale of ≈ 3 years), a narrow-line quasar at z=0.400. We found evidence for a steep continuum and a relativistic iron K_α emission line, which are both accounted for in the framework of either ionized reflection or partial-covering of the source. The large EW (3.1 ± 0.8 keV in the source rest frame) of the line would be naturally explained in the context of ionized reflection if the source of X-ray photons is very close to the accreting black hole, thus being subject to strong gravity effects; however, a partial covering model cannot be ruled out on the basis of the current data. The steep X-ray spectrum is possibly related to the high accretion rate of PG 1543+489, as suggested by recent studies on quasars and, likely, by the strong outflow and asymmetric profiles measured in the [O III] 5007Å and C IV 1549Å emission lines, which make of PG 1543+489 one of the most intriguing quasars in the PG sample and a valuable scientific case for future investigations.

ACKNOWLEDGMENTS

CV, EP and SB thank for support the Italian Space Agency (contracts ASI–INAF I/023/05/0 and ASI I/088/06/0); GM acknowledges support from the UK PPARC. The authors thank J. Fritz, M. Meneghetti, M. Mignoli, L. Moscardini, G. Ponti and O. Shemmer for useful discussions, and the anonymous referee for his/her useful comments and suggestions which improved the quality of the paper.

REFERENCES

Anders E., Grevesse N., 1989, Geochim. Cosmochim. Acta, 53, 197
Aoki K., Kawaguchi T., Ohta K., 2005, ApJ, 618, 601
Arnaud K.A., 1996, in Jacoby G., Barnes J., eds, ASP Conf. Ser. Vol. 101, Astronomical Data Analysis Software and Systems V. Astron. Soc. Pac., San Francisco, p. 17
Avni Y., 1976, ApJ, 210, 642
Baldi A., Molendi S., Comastri A., Fiore F., Matt G., Vignali C., 2002, ApJ, 564, 190
Baskin A., Laor A., 2005, MNRAS, 356, 1029
Boller T., 2004, Progress of Theoretical Physics Supplement, 155, 217
Boller T., Brandt W.N., Fink H., 1996, A&A, 305, 53
Boroson T.A., 2002, ApJ, 565, 78
Boroson T.A., Green R.F., 1992, ApJS, 80, 109
Brandt W.N., Boller T., 1998, Astron. Nachr., 319, 163
Brandt W.N., Mathur S., Elvis M., 1997, MNRAS, 285, L25
Brocksopp C., Starling R.L.C., Schady P., Mason K.O., Romero-Colmenero E., Puchnarewicz E.M., 2006, MNRAS, 366, 953
Chartas G., Eracleous M., Dai X., Agol E., Gallagher S., 2007, ApJ, 661, 678
Comastri A., Brusa M., Civano F., 2004, MNRAS, 351, L9
Crummy J., Fabian A.C., Brandt W.N., Boller T., 2005, MNRAS, 361, 1197
Crummy J., Fabian A.C., Gallo L., Ross R.R., 2006, MNRAS, 365, 1067
Dabrowski Y., Lasenby A.N., 2001, MNRAS, 321, 605
Dai X., Chartas G., Eracleous M., Garmire G.P., 2004, ApJ, 605, 45
D'Elia V., Padovani P., Landt H., 2003, MNRAS, 339, 1081
Dickey J.M., Lockman F.J., 1990, ARA&A, 28, 215
Done C., 2007, Progress of Theoretical Physics Supplement, "The Extreme Universe in the *Suzaku* Era", 169, 248
Elvis M., et al., 1994, ApJS, 95, 1
Fabian A.C., Rees M.J., Stella L., White N.E., 1989, MNRAS, 238, 729
Fabian A.C., Ballantyne D.R., Merloni A., Vaughan S., Iwasawa K., Boller T., 2002, MNRAS, 331, L35
Fabian A.C., Miniutti G., Gallo L., Boller T., Tanaka Y., Vaughan S., Ross R.R., 2004, MNRAS, 353, 1071
Gabriel C., et al., 2004, ASP Conf. Ser. Vol. 314, Astronomical Data Analysis Software and Systems XIII, p. 759
Gallo L.C., Boller T., Brandt W.N., Fabian A.C., Grupe D., 2004a, MNRAS, 352, 744
Gallo L.C., Tanaka Y., Boller T., Fabian A.C., Vaughan S., Brandt W.N., 2004b, MNRAS, 353, 1064
George I.M., Turner T.J., Yaqoob T., Netzer H., Laor A., Mushotzky R.F., Nandra K., Takahashi T., 2000, ApJ, 531, 52
Guainazzi M., Bianchi S., Dovčiak M., 2006, Astron. Nachr., 88, 789
Kaspi S., Smith P.S., Netzer H., Maoz D., Jannuzi B.T., Giveon U., 2000, ApJ, 533, 631
Komossa S., Xu D., Zhou H., Storchi-Bergmann T., Binette L., 2008, ApJ, in press (arXiv:0803.0240)
Krumpe M., Lamer G., Schwope A.D., Husemann B., 2007, A&A, 470, 497
Inoue H., Terashima Y., Ho L.C., 2007, ApJ, 662, 860
Iwasawa K., Fabian A.C., Mushotzky R.F., Brandt W.N., Awaki H., Kunieda H., 1996, MNRAS, 279, 837
Jiménez-Bailón E., Piconcelli E., Guainazzi M., Schartel N., Rodríguez-Pascual P.M., Santos-Lleó M., 2005, A&A, 435, 449
Just D.W., Brandt W.N., Shemmer O., Steffen A.T., Schneider D.P., Chartas G., Garmire G.P., 2007, ApJ, 665, 1004
Laor A., 1991, ApJ, 376, 90
Laor A., Fiore F., Elvis M., Wilkes B.J., McDowell J.C., 1994, ApJ, 435, 611
Laor A., Fiore F., Elvis M., Wilkes B.J., McDowell J.C., 1997, ApJ, 477, 93
Longinotti A.L., Sim S.A., Nandra K., Cappi M., 2007, MNRAS, 374, 237
Maiolino R., Marconi A., Salvati M., Risaliti G., Severgnini P., Oliva E., La Franca F., Vanzi L., 2001, A&A, 365, 28
Malzac J., Merloni A., Suebsuwong T., 2006, Astron. Nachr., 88, 789
Marconi A., Risaliti G., Gilli R., Hunt L.K., Maiolino R., Salvati M., 2004, MNRAS, 351, 169
Marziani P., Zamanov R., Sulentic J.W., Calvani M., 2003a, MNRAS, 345, 1133
Marziani P., Zamanov R., Sulentic J.W., Calvani M., Dultzin-Hacyan D., 2003b, MmSAI, 74, 492
Matsumoto C., Leighly K.M., Kawaguchi T., 2006, ESASP, 604, 503
Matt G., Fabian A.C., Reynolds C.S., 1997, MNRAS, 289, 175
Merloni A., Malzac J., Fabian A.C., Ross R.R., 2006, MNRAS, 370, 1699

Mineo T., et al., 2000, A&A, 359, 471
Miniutti G., Fabian A.C., 2004, MNRAS, 349, 1435
Miniutti G., Fabian A.C., 2006, MNRAS, 366, 115
Miniutti G., Fabian A.C., Goyder R., Lasenby A.N., 2003, MNRAS, 344, L22
Miniutti G., Fabian A.C., Miller J.M., 2004, MNRAS, 351, 466
Miniutti G., Ponti G., Dadina M., Cappi M., Malaguti G., 2006, MNRAS, 375, 227
Nandra K., George I.M., Mushotzky R.F., Turner T.J., Yaqoob T., 1997, ApJ, 477, 602
Nandra K., George I.M., Mushotzky R.F., Turner T.J., Yaqoob T., 1999, ApJ, 523, L17
Nandra K., O'Neill P.M., George I.M., Reeves J.N., Turner T.J., 2006, Astron. Nachr., 88, 789
Nandra K., O'Neill P.M., George I.M., Reeves J.N., 2007, MNRAS, 382, 194
Netzer H., Trakhtenbrot B., 2007, ApJ, 654, 754
Page K.L., Turner M.J.L., Reeves J.N., O'Brien P.T., Sembay S., 2003, MNRAS, 338, 1004
Page K.L., Reeves J.N., O'Brien P.T., Turner M.J.L., 2005, MNRAS, 364, 195
Piconcelli E., Cappi M., Bassani L., Di Cocco G., Dadina M., 2003, A&A, 412, 689
Piconcelli E., Jimenez-Bailón E., Guainazzi M., Schartel N., Rodríguez-Pascual P.M., Santos-Lleó M., 2005, A&A, 432, 15
Piconcelli E., et al., 2006, A&A, 453, 839
Ponti G., Miniutti G., Cappi M., Maraschi L., Fabian A.C., Iwasawa K., 2006, MNRAS, 368, 903
Porquet D., 2006, A&A, 445, L5
Porquet D., Reeves J.N., 2003, A&A, 408, 119
Porquet D., Reeves J.N., O'Brien P., Brinkmann W., 2004, A&A, 422, 85
Pounds K.A., Done C., Osborne J.P., 1995, MNRAS, 277, L5
Protassov R., van Dyk D.A., Connors A., Kashyap V.L., Siemiginowska A., 2002, ApJ, 571, 545
Puchnarewicz E.M., Mason K.O., Siemiginowska A., Pounds K.A., 1995, MNRAS, 276, 20
Reeves J.N., Turner M.J.L., 2000, MNRAS, 316, 234
Reynolds C.S., 1997, MNRAS, 286, 513
Richards G.T., et al., 2006, ApJS, 166, 470
Ross R.R., Fabian A.C., 2005, MNRAS, 358, 211
Saez C., Chartas G., Brandt W.N., Lehmer B.D., Bauer F.E., Dai, X., Garmire G.P., 2008, AJ, 135, 1505
Schartel N., Rodríguez-Pascual P.M., Santos-Lleó M., Ballo L., Clavel J., Guainazzi M., Jiménez-Bailón E., Piconcelli E. 2007, A&A, 474, 431
Schmidt M., Green R.F., 1983, ApJ, 269, 352
Shemmer O., Netzer H., Maiolino R., Oliva E., Croom S., Corbett E., di Fabrizio L., 2004, ApJ, 614, 547
Shemmer O., Brandt W.N., Vignali C., Schneider D.P., Fan X., Richards G.T., Strauss M.A., 2005, ApJ, 630, 729
Shemmer O., Brandt W.N., Netzer H., Maiolino R., Kaspi S., 2006, ApJ, 646, L29
Shemmer O., Brandt W.N., Netzer H., Maiolino R., Kaspi S., 2008, ApJ, in press (arXiv:0804.0803)
Spergel D.N. et al., 2003, ApJS, 148, 175
Tanaka Y., et al., 1995, Nature, 375, 659
Vestergaard M., Peterson B.M., 2006, ApJ, 641, 689
Vignali C., Brandt W.N., Schneider D.P., Kaspi S., 2005, AJ, 129, 2519
Weaver K.A., Krolik J.H., Pier E.A., 1998, ApJ, 498, 213
Zamanov R., Marziani P., Sulentic J.W., Calvani M., Dultzin-Hacyan D., Bachev R., 2002, ApJ, 576, L9